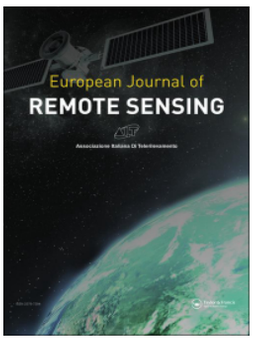

European Journal of Remote Sensing

ISSN: (Print) (Online) Journal homepage: https://www.tandfonline.com/loi/tejr20

Land cover change across 45 years in the world's largest mangrove forest (Sundarbans): the contribution of remote sensing in forest monitoring

Kanan Akbar Hossain, Mauro Masiero & Francesco Pirotti

To cite this article: Kanan Akbar Hossain, Mauro Masiero & Francesco Pirotti (2022): Land cover change across 45 years in the world's largest mangrove forest (Sundarbans): the contribution of remote sensing in forest monitoring, European Journal of Remote Sensing, DOI: 10.1080/22797254.2022.2097450

To link to this article: https://doi.org/10.1080/22797254.2022.2097450

Published online: 13 Jul 2022.

EUROPEAN JOURNAL OF REMOTE SENSING
https://doi.org/10.1080/22797254.2022.2097450

Taylor & Francis
Taylor & Francis Group

Land cover change across 45 years in the world's largest mangrove forest (Sundarbans): the contribution of remote sensing in forest monitoring

Kanan Akbar Hossain [a], Mauro Masiero [a] and Francesco Pirotti [a,b]

[a]Department of Land, Environment, Agriculture and Forestry, University of Padova, Padova, Italy; [b]CIRGEO Interdepartmental Research Center of Geomatics, University of Padova, Padova, Italy

ABSTRACT

This study explored the land use land cover (LULC) change over 45 years (1975 -2020) in the world's largest mangrove forest, Sundarbansusing Landsat imagery. LULC maps were created with same-season imagery with the lowest cloud cover at four intervals: 1975, 1990, 2005, and 2020. Maximum likelihood classification (MLC) was applied to assign five classes: dense forest, moderate forest, sparse forest, barren land, and water body. Accuracy assessment was carried out with 250 control points for each year resulting in overall accuracy and kappa coefficient ranging from 84.8% to 90.0% and 0.81 to 0.87, respectively. Results show dense forest at its highest cover in 1975 and then decreasing by an estimated annual rate of 1.3% from 1975 to 2020, but not consistently. Dense forest class mostly turned moderate and sparse; most of the sparse forest class turned to barren land. Most of the barren lands were located near the boundary between forest and human settlement, and these two classes were more frequent in the Indian part of Sundarbans than in the Bangladesh part. The conclusion is that the time-series of remote sensing data can validly support effective forest management by identifying space and time changes in the biodiversity of Sundarbans.

ARTICLE HISTORY
Received 13 October 2021
Revised 10 May 2022
Accepted 30 June 2022

KEYWORDS
Sundarbans mangrove; Landsat; LULC; accuracy assessment; anthropogenic disturbances; cyclonic storms; climate change

Introduction

Mangroves forests are found in the tropical and sub-tropical areas of the world and create a forest in the intertidal region between sea and land (Datta & Deb, 2012; FAO, 2010; Islam et al., 2019). About 41% of the world's mangroves are distributed in South and Southeast Asia, with the remaining 59% shared by other regions (Malik et al., 2017). Sundarbans is the largest contiguous mangrove forest of the world; it alone constitutes 3% of the global mangroves forest area (Chanda et al., 2016), covering 10,000 km^2, of which 62% (6,200 km^2) are placed in Bangladesh and the rest 38% (3800 km^2) in India (Ghosh et al., 2015). The Sundarbans are managed independently by Bangladesh and India, but they were considered as a single entity until the partition of India in 1947 (Ortolano et al., 2016).

Sundarbans provide habitat for numerous wild fauna and flora, essential to maintaining coastal biodiversity and ecological integrity (Barbier, 2007). In addition, this forest includes hosting many threatened and endangered species, such as the Royal Bengal tiger, estuarine crocodile, Indian python, and some species of river dolphins (Ortolano et al., 2016). Therefore, Sundarbans is considered a hotspot for biodiversity conservation, and at the same time, an important provider of a wide range of ecosystem services (FAO, 2010; Payo et al., 2016). About 3.5 million Bangladeshi and 4 million Indian people are directly or indirectly dependent on these ecosystem services for livelihood and socio-economic well-being (Giri et al., 2007; Kibria et al., 2018; Ortolano et al., 2016; Roy et al., 2013). Most importantly, Sundarbans protect millions of coastal people and their resources from storms, cyclones, and coastal soil erosion. Moreover, the carbon sequestration rate of mangrove forests is four times higher than other tropical forests (Donato et al., 2011). Accordingly, Sundarbans is an important hub to store total ecosystem carbon that reduces greenhouse gas emissions. Recognizing the significance and uniqueness of the Sundarbans ecosystem, the Sundarbans National Park (SNP) in India and the Sundarbans Reserve Forest (SRF) in Bangladesh have been declared World Heritage Sites by the United Nations Educational, Scientific and Cultural Organization (UNESCO) in 1987 and 1997, respectively. SRF was also included as a Ramsar site in 1992 (Ghosh et al., 2015; Quader et al., 2017; Rahman et al., 2015).

Sundarbans mangroves in Bangladesh and India are decreasing at an alarming rate due to natural and anthropogenic causes. Giri et al. (2007) reported that the Sundarbans mangrove forest area decreased by 1.2% from 1970 to 2000. The degradation is due to overexploitation of Non-Timber Forest Products (NTFPs), expansion of agricultural (shrimp farming

CONTACT Francesco Pirotti francesco.pirotti@unipd.it Department of Land, Environment, Agriculture and Forestry, University of Padova, Padova, Italy

and paddy cultivation) and industrial activities (power plant, shipyard, oil spills from boats and ships, dam construction, and so on) sea level rise, salinity, siltation, cyclones, and storm surges (Gopal & Chauhan, 2006; Islam, 2010). Sea level rise is considered the most significant climate change-related threat to Sundarbans mangrove regions (Loucks et al., 2010; Quader et al., 2017; Rahman, 2020). For instance, sea level rise adjacent to the Sundarbans is +3.90 ± 0.46 mm/year (Nishat et al., 2019), and 40–60% of mangrove area will decrease if sea-level rise will grow up to 1 m (Rahman et al., 2015, World bank, 2010). Neogi et al. (2017) also studied that cyclonic storms are increased by 26% from 1881 to 2001 towards the Sundarbans coastal area. However, Das and Datta (2016) reported that anthropogenic activities are one of the major causes of the ecological degradation of Sundarbans. For instance, freshwater discharge of the Ganges waterway was decreased from 3700 m^3s^{-1} in 1962 to 364 in 2006 due to the construction of the Farakka Barrage in 1975, which led to increasing salinity level of the Sundarbans (Islam & Gnauck, 2008). Moreover, Bangladesh and Indian governments recently agreed to build a coal-fed thermal power plant in Rampal 14 km north of the Sundarbans is an additional threat for biodiversity and forest-dependent people.

The Sundarbans' ecological and socio-economic perspectives are a single unit (Ortolano et al., 2016), but the legal borderline and different management policies between Bangladesh and India make it difficult to provide an overview regarding the evolution and current state of the entire Sundarbans (Giri et al., 2014; Gopal & Chauhan, 2006; Ishtiaque & Chhetri, 2016). In addition to this, vast of the Sundarbans areas are inaccessible are due to forest geophysical features and other environmental factors (Datta & Deb, 2012; Emch & Peterson, 2006). In this situation, remote sensing is useful for detecting and monitoring spatio-temporal changes e.g. LULC change and specifically forest mapping (LaRocque et al., 2020; Vaglio Laurin et al., 2016) in and around the Sundarbans (Quader et al., 2017; Rahman, 2013). Dahdouh-Guebas et al. (2004) reported that optical remote sensing with moderate-to-high spatial resolution is a reliable tool for mapping and characterizing mangrove ecosystems. Rahman et al. (2010) also reported that the monitoring, analysis, and modeling of LULC are significant for Sundarbans' conservation and management planning. Therefore, remote sensing help in the decision-making of forest management policies (Pirotti et al., 2014) as well as in achieving some United Nations Sustainable Development Goals (UN-SDGs) (Chirici, 2020). However, there have been insufficient studies undertaken in Sundarbans, particularly in Bangladesh Sundarbans, to track and discuss the numerous causes of LULC change (Hasan et al., 2020; Islam et al., 2019). In addition, most of these studies conclude by highlighting limitations and suggest that further investigation is required (Quader et al., 2017). For instance, the majority of the limitations regarding image selection and image pre-processing have been recently addressed by archives which provide corrected and analysis-ready data, but often area-specific image selection and processing is necessary. Another aspect is that rigorous accuracy assessment, and applying these workflow consistently is essential to assess LULC accurately (Congalton, 1991; Rwanga & Ndambuki, 2017). In our study, we try to fill these knowledge gaps to detect the periodic changes of Sundarbans.

The general objective of our work is to explore the spatio-temporal changes of the entire Sundarbans (including both Bangladesh and Indian parts) through remotely sensed data from 1975 to 2020. To achieve this, we have addressed the following specific objectives: (1) measuring accuracy of the classified LULC classes (2) mapping and assessing the different LULC (3) thematic change and (4) positive, negative and unchanged areas over 45 years. To our knowledge, a study with these spatial and temporal scales has not been carried out in the region.

Study area

We considered the entire Sundarbans Mangrove forest (including Bangladesh and Indian part) as a study area, which is located between 21°32′ and 22°40′ N and 88°05′ and 89°51′ E (Figure 1). The Sundarbans are formed on the estuary created by the Hooghly, Ganges, Brahmaputra, and Meghna rivers in the Bay of Bengal. These rivers are the main sources to supply freshwater and sediments to Sundarbans. The average elevation of Sundarbans is about 2 m above the mean sea level (Payo et al., 2016). Approximately 30% of areas of the Sundarbans are covered by water which is shaped by numerous rivers, canals, and tidal flows (Nishat et al., 2019). The tide inundated the forest twice a day (Barlow et al., 2011), and was characterized by a tropical climate with a dry season during December–February and a monsoonal wet season during March–November (Quader et al., 2017). Seasonal mean minimum and maximum temperatures vary from 12°C to 24°C and 25°C to 35°C, respectively. The total annual amount of precipitation is between 1500 mm to 2000 mm. During the monsoon period, the tropical cyclones always hit the Sundarbans, causing severe flooding and wind damage (Ghosh et al., 2015).

Methodology

The study of spatio-temporal changes for an extended period and larger areas are challenging regarding images collection from multiple sensors, processing, correction, and accuracy assessment (Roy & Inamdar, 2019). Our study area is covered by the numerous satellite scenes from various sensors from 1975 to 2020. Therefore, we designed the study in

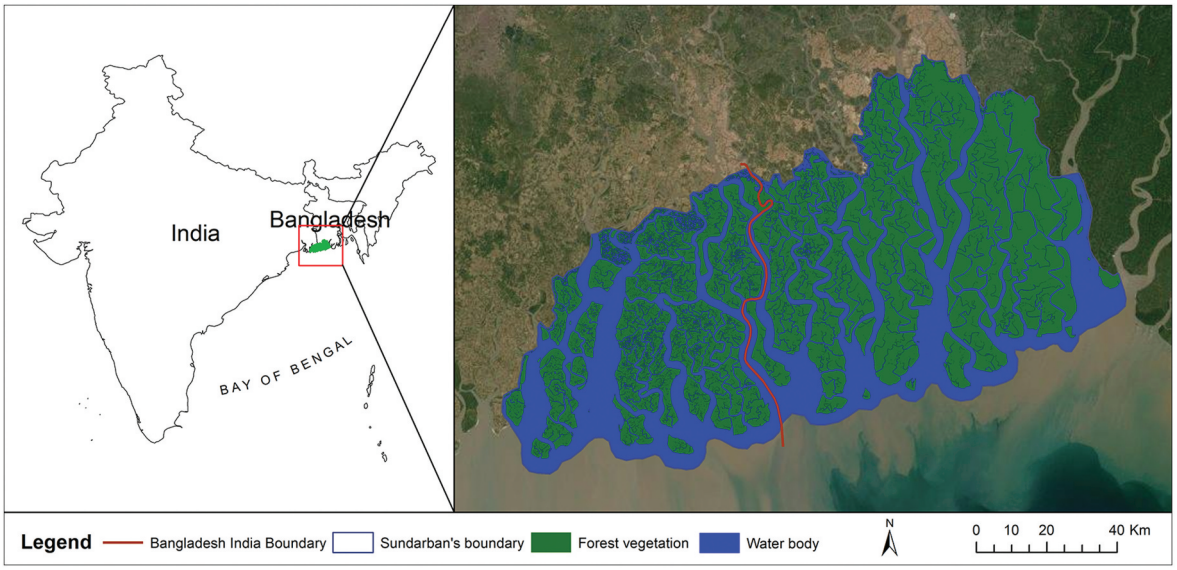

Figure 1. Sundarbans Mangrove forest (study area).

a sequential framework to ensure the best accuracy, which includes: i) image collection, ii) image pre-processing, iii) image classification, (iv) accuracy assessment, and (v) final mapping (Figure 2).

Image collection

Landsat satellite "collection-1 level-1" images were used to explore the LULC of Sundarbans from 1975 to 2020. The United States Geological Survey USGS (2019) reported that the Landsat "collection-1 level-1" images are the best-known quality to support time series analysis. Except for one, all these cloud-free images were acquired from January to February from the USGS. January and February are the winter season (cold-dry condition) and less cloudy in Sundarbans regions; therefore, there is no significant variation in vegetation phenology and spectral signature between these two months (Bera & Chatterjee, 2019; Islam et al., 2019).

The 2020 images were from the Operational Land Imager (OLI) and Thermal Infrared Sensor (TIRS). The rest of the images were from Landsat Thematic Mapper (TM) and Landsat Multi-Spectral Scanner (MSS). In the case of 1975, three adjacent Landsat images are needed to cover the entire Sundarbans. The source and other specifications of the used satellite images of Sundarbans are given in Table 1.

Image pre-processing

Atmospheric and radiometric correction of collected images were completed using Fast Line-of-sight Atmospheric Analysis of Hypercubes (FLAASH) in ENVI 5.3. FLAASH is a highly established and advanced atmospheric correction algorithm in remote sensing platforms (Serrano et al., 2016). Although FLAASH technique requires longer processing times, it generally provides more accurate results than other methods (Smith, 2015). The FLAASH model includes a method (Equation 1 and 2) for minimizing the inconsistency of

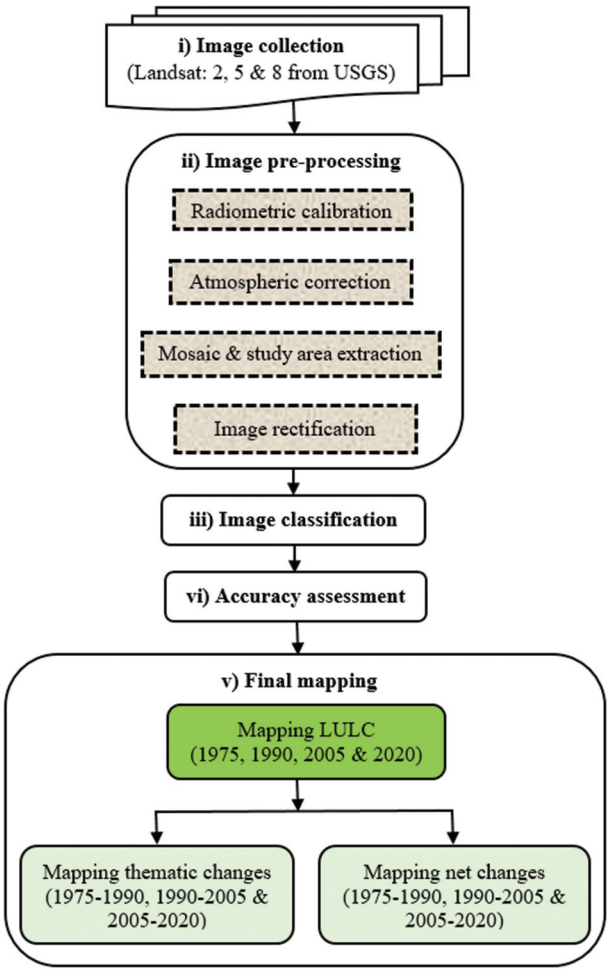

Figure 2. Frame work of methodological activities followed in the study.

Table 1. Source and specification of satellite images used in the study.

Year	Data acquisition date/time	SatelliteSensor	Path/ Row	Used bands	Spatial resolution	Cloud cover	Covered area*
1975	19 February 1975	L 2 MSS	147/045	4–7	60 m	0%	BS
	10 January 1976	L 2/MSS	148/045	4–7	60 m	0%	IS, BS
	10 January 1976	L 2/MSS	148/044	4–7	60 m	0%	BS
1990	24 February 1990	L 5/TM	137/045	1–7	30 m	0%	BS
	14 January 1990	L 5/TM	138/045	1–7	30 m	0%	IS, BS
2005	16 January 2005	L 5/TM	137/045	1–8	30 m	0%	BS
	7 January 2005	L 5/TM	138/045	1–8	30 m	0%	IS, BS
2020	26 January 2020	L 8/OLI	137/045	1–7	30 m	0%	BS
	Jan 17, 2020	L 8/OLI	138/045	1–7	30 m	0.62%	IS, BS

Covered area*: BS = Bangladesh Sundarbans, IS = Indian Sundarbans

radiometric and atmospheric (i.e. water vapor, haze, smoke, fog, dust and aerosol) effect in images (Kaufman et al., 1997; Matthew et al., 2000). The first term in Equation (1) measure the radiance that is reflected from the surface and travels directly into the sensor, while the second term corresponds to radiance from the surface that is scattered by the atmosphere into the sensor.

$$L = \left(\frac{A}{1-\rho e S}\right) + \left(\frac{A_e}{1-\rho e S}\right) + La \quad (1)$$

Where, L is the spectral radiance at sensor pixel, ρ is the pixel surface reflectance, $_e$ is an average surface reflectance for the pixel and a surrounding region, S is the spherical albedo of the atmosphere, La is the radiance back-scattered by the atmosphere, A and B are coefficients that depend on atmospheric and geometric conditions but not on the surface.

Geometrically, our study area is almost flat, where A, B, S, and La are strongly dependent on the atmospheric conditions (e.g. water vapor). Therefore, the equation (1) is resolved for the pixel surface reflectance in all of the sensor channels. The solution process includes calculating a spatially averaged radiance image Le, from which the spatially averaged reflectance ρ_e is estimated using the approximate equation (2).

$$L_e \approx \left[\frac{(A+B)_{\rho e}}{1-\rho e S} + L_a\right] \quad (2)$$

We also applied the modified pseudo-invariant features (PIF) method as part of the relative radiometric correction of the scenes of the Landsat sensor (Myeong et al., 2006). The PIF method reduces the inconsistency between different scenes of the same mosaic of images (Quader et al., 2017). After mosaicking, the images of the study area were extracted by considering the administrative boundary of Sundarbans.

For image rectification, we used about 50 ground control points and the dispersed ground control points generated a root mean square error (RMSE) using Equation (3).

$$RMSE = \sqrt{\frac{\sum_{i=1}^{n} (y_i - x_i)^2}{n}} \quad (3)$$

Where, y_i is the observed sample points, x_i is the predicted sample points and, n is the total number of observations. The square of the difference (y-x) always consists in a value of one when it is an error, and zero when it is correct. So the RMSE is the square root of the misclassification rate, and the lower RMSE stands the higher the accuracy of LULC prediction (Talukdar et al., 2020). In this study, maximum RMSE was found 0.39 that belong to the acceptable range for LULC change detection (Knorn et al., 2009; Tucker et al., 2004). After that the images were resampled to a 30 m pixel size using the nearest neighbour resampling method (Ghosh et al., 2016).

Image classification

A variety of image classification techniques are used for mapping and studying LULC change (Billah et al., 2021; Lu & Weng, 2007). We performed supervised maximum likelihood classification (MLC) on the study area at four time periods over 45 years (1975, 1990, 2005, and 2020). The classification was assigned to five classes: dense/moderate/sparse forest, barren land, and water. Supervised MLC classification techniques have been used worldwide over the last two decades to study mangrove LULC (Bera & Chatterjee, 2019; Giri et al., 2007; Chen et al., 2013; Giri & Muhlhausen, 2008; Giri et al., 2010; Islam et al., 2019; Jones et al., 2016; Ghosh et al., 2016; Kumar et al., 2021; Pham & Yoshino, 2015). Because, the MLC algorithm is one of the most well-known parametric classifiers used for supervised classification (Li et al., 2014) and is easy to use, thus, an extended training process is not required (Chen et al., 2013; Datta & Deb, 2012). Moreover, the MLC algorithm reduces the data necessities and provides a potential to extract comprehensive information (Hassan, 2017; Jat et al., 2017) by calculating the weighted distance or likelihood of an unknown measurement vector that belongs to one of the known classes, based on the Bayesian equation. The unknown measurement vector is assigned to the class based on the highest probability of fit. Consideration of a variance-covariance matrix within the class distributions is considered one of the advantages of this algorithm (Ghosh et al., 2016). However, a sufficient number of training samples are prerequisites for a successful and

superior classification (Lu & Weng, 2007). For each study year, we selected a total of 245 training samples throughout the area to identify the LULC classes (a total of 980 training samples for four study years). The training samples were distributed among the LULC classes as follows: 50 samples for dense forest, 50 for moderate dense forest, 45 for sparse forest, 35 for barren land, and 65 for water body. The water color is different near the coastal/beach/shoreline areas than the deep river basins of Sundarbans due to the sedimentation, water deepness, and tidal effect; thus, the spectral variation is a little different. In this case, we considered a large number of water body sites for training samples. The training samples were selected manually from the images for accurate classification by careful inquiry of homogeneous pixels of these five LULC classes (Islam et al., 2019). Moreover, we used high-resolution Google Earth images as a reference point to identify the actual LULC classes (Figure 3).

Accuracy assessment

For accuracy assessment, we randomly selected 250 control points for each study year over the classified images (a total of 1000 control points for four study years). The points were labelled according to the land cover around a 30 m radius – in case a point fell too close between two different land cover classes, it was slightly shifted in order to make sure that it is representative of a full Landsat pixel. These control points were verified using Google Earth historical images. However, no information is available in Google Earth historical images for the year 1975. Therefore, for this year, we verified images using previous literature, expert-based information (Quader et al., 2017), and with historical toposheet map (sheet NF 45–8, series U 502) from the survey of India. Classification accuracy for the classified images was assessed by computing error metrics (producer, user and overall accuracy) and kappa coefficients (K) (Kanniah et al., 2015; Stehman, 1996). The calculation of K is described in equations (4).

$$K = \frac{\left[n\sum_{i=1}^{r} x_{ij} - \sum_{i=1}^{r}(x_i x_j)\right]}{\left[n^2 - \sum_{i=1}^{r}(x_i x_j)\right]} \quad (4)$$

Where, n is the total of sample, x_{ij} is the total corrected sample, x_i is the producer total and x_j is the user total. The value of K equal to one means perfect agreement, whereas a value close to zero means that the agreement is no better than would be expected by chance (Rwanga & n.d. ambuki, 2017). Therefore, higher value of K indicates the higher the accuracy of LULC expectation.

Final mapping

After the accuracy assessment, the final map was completed for four different study years (1975, 1990, 2005, and 2020) to estimate different LULC. Then, we calculated periodic LULC, thematic and difference from one year to another. Finally, the causes of periodic change patterns were discussed in terms of human induced (i.e. agricultural and industrial activities) and climate change-related impacts (i.e. cyclonic storms and sea level rise).

Results

Accuracy assessment

The accuracy assessment results of the classified images show that the overall accuracy ranges were between 84.8% and 90.0% from 1975 to 2020. The highest and lowest overall accuracy was found for

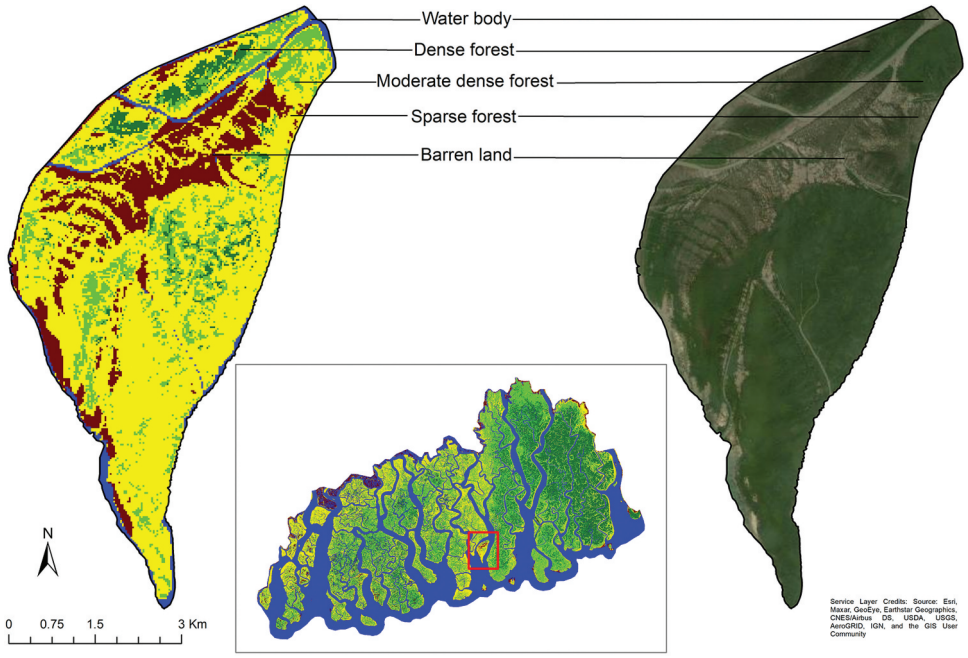

Figure 3. Image classification and accuracy assessment.

Table 2. Analysis accuracy metrics of classified Landsat images of Sundarbans (1975–2020).

	Land use classes											
	Dense forest		Medium dense forest		Sparse forest		Barren land		Water body			
Year(Used sensor)	PA	UA	PA	UA	PA	UA	PA	UA	PA	UA	Overall accuracy	Kappa coefficient (K)
1975 (MSS)	87	84	82	83	81	84	79	83	92	91	84	0.81
1990 (MSS)	88	87	81	87	84	89	88	93	91	90	88	0.85
2005 (TM)	89	90	80	86	82	87	85	90	94	91	87	0.83
2020 (OLI)	88	90	86	88	89	85	80	89	96	93	90	0.87

"PA" and "UA" indicates producer's and user's accuracy respectively

2020 and 1975, respectively (Table 2). The producer's (PA) and user's (UA) accuracy were highest for water, and the differences between these values (PA and UA) were less than other LULC classes. The maximum differences between producer's and user's values were found for the sparse and moderate forest. The kappa coefficient ranges were from 0.81 to 0.87 from 1975 to 2020 (Table 2). The kappa value was highest for the year 2020 than others periods.

Land use land cover change

The LULC maps of our study revealed that in 1975 the dense forest covered maximum areas (45%) of Sundarbans (Figure 4). The second main class cover was water (32%), followed by barren land (10%), moderate dense (8%), and sparse forest (5%) (Table 3). However, in 1990 and 2005, the water covered maximum areas instead of dense forest, and the other land cover was followed by moderate dense forest, sparse forest, and barren land. In 2020, most areas were covered by water and moderate dense forest where the dense forest was replaced with third position (Figure 5). Our geo-spatial maps also showed that most of the dense forest occupied the eastern part of Sundarbans from 1975 to 2020. The sparse forest and barren land areas were highest in the Indian part of Sundarbans than in Bangladesh ones. However, the maximum barren land areas are located near to borderline between forest and human habitat (Figure 4).

The study showed that in the overall study timespan, there was a rate of 1.3% of dense forest loss per year from 1975 to 2020 (Table 3), but not consistently. The dense forest cover decreased from 1975 to 1990 and 2005 to 2020 with an annual rate of 2.75% and 2.25%, respectively. However, the dense forest

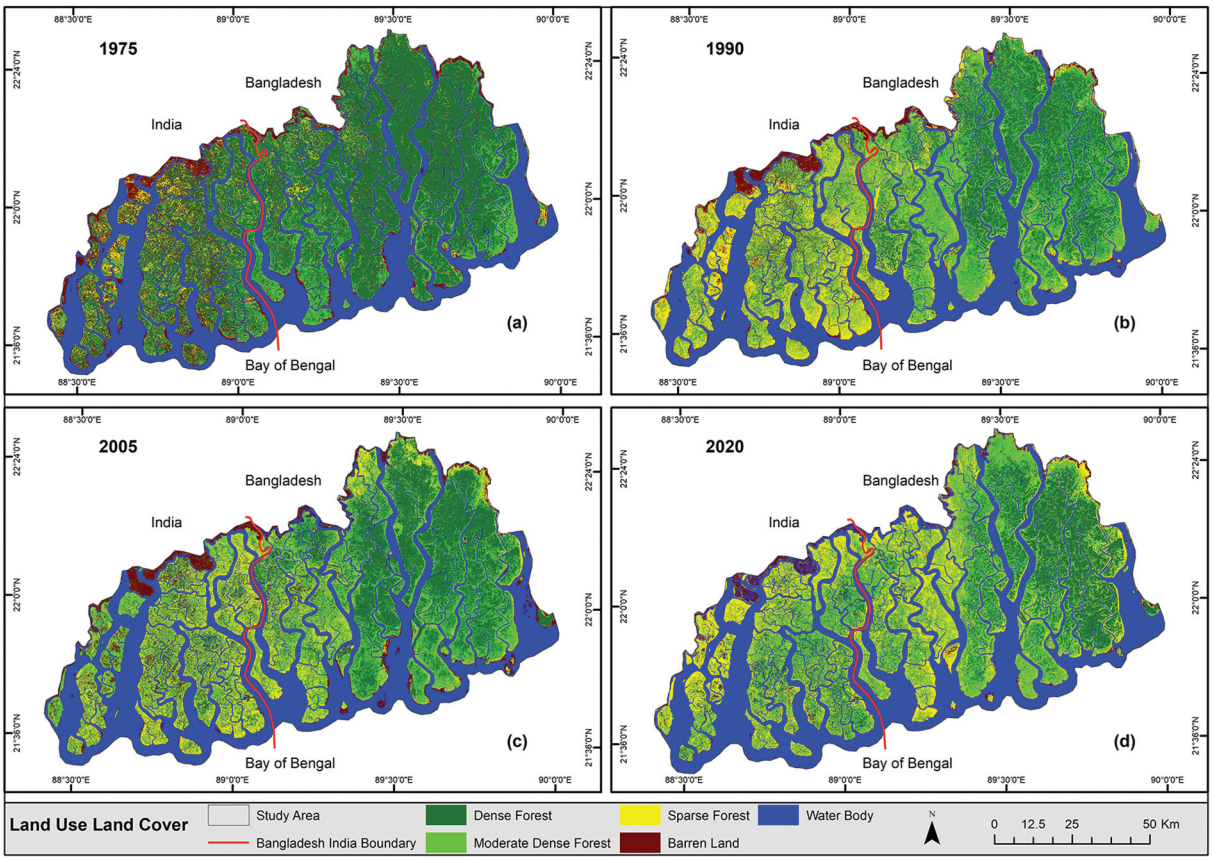

Figure 4. LULC of Sundarbans from 1975 to 2020.

Table 3. Analysis LULC of Sundarbans (1975–2020).

	Area (km^2)(% of total area)				Area changes (km^2)(Annual rate of changes %)			
LULC	1975	1990	2005	2020	1975–1990	1990–2005	2005–2020	1975–2020
Dense forest	4527(45%)	2657(27%)	2818(28%)	1864(19%)	−1870(−2.75%)	+161(+0.40%)	−954(−2.25%)	−2663(−1.30%)
Moderate – dense forest	809(8%)	1817(18%)	1734(17%)	2120(21%)	+1008(+8.31%)	−83(−0.30%)	+386(+1.48%)	+1312(+3.61%)
Sparse forest	530(5%)	1735(17%)	1363(14%)	1815 (18%)	+1205(+15.15%)	−372(−1.43%)	+452(+2.21%)	+1285(+5.39%)
Barren land	1002(10%)	416(4%)	522(5%)	247 (2%)	−585(−3.90%)	+106(+1.70%)	−275(−3.51%)	−754(−1.67%)
Water bodies	3142(32%)	3408(34%)	3596(36%)	3963 (40%)	+266(+0.57%)	+188(+0.37%)	+366(+0.68%)	+821(+0.58%)

"+" and "−" indicates increase and decrease respectively

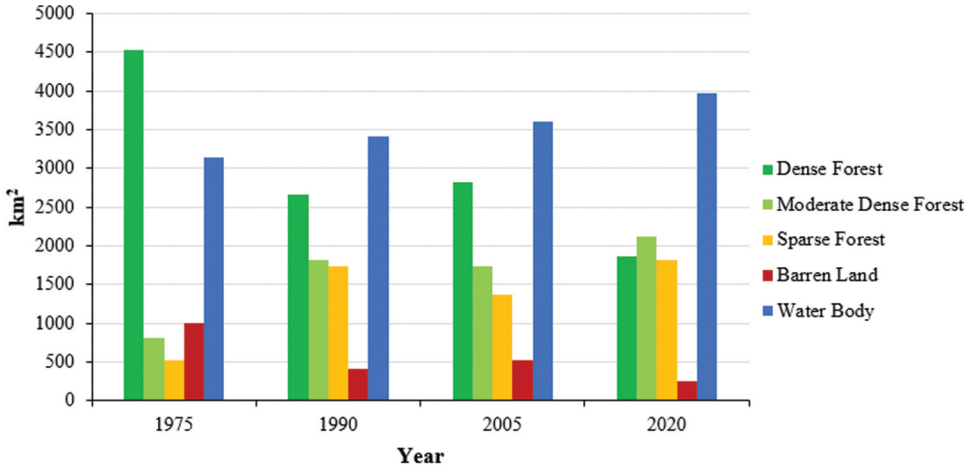

Figure 5. Change areas by different LULC of Sundarbans from 1975 to 2020.

increased by giving a yearly rate of 0.40% from 1990 to 2005. Moderate and sparse forests increased from 1975 to 2020, but these two types of forests decreased from 1990 to 2005. The increasing annual rates of moderate dense and sparse forest were greater than the dense forest from 1975 to 2020, which indicates the degradation of forest areas by converting dense forest into moderate dense and then sparse forest. The water body always increased gradually (Figure 5) by giving an annual rate of 0.6% from 1975 to 2020, but the increasing trend was highest for the last 15 years (2005 to 2020) (Table 3).

Thematic changes

The thematic change map provides information that the significant areas of dense forest were altered by sparse and moderate dense forest from 1975 to 2020 (Figure 6). But, the alternation between these types of forest cover was higher from 1975 to 1990. Moreover, the map shows that the areas of sparse, moderate, and dense forest were increased by reducing barren areas in the Indian part of Sundarbans from 1975 to 2020, whereas Bangladesh Sundarbans increased sparse and moderate dense forest by reducing dense forest areas. The areas of barren land were decreased from 1975 to 2020. However, the barren areas located between forest boundary and human settlement were unchanged (Figure 6).

The results of our finding showed that most of the thematic changes were found for the dense forest in the last 45 years (1975 to 2020), where significant areas of the dense forest turned into moderate dense (15.62%), sparse forest (10.41%) and water bodies (2.45%) (Table 4). The dense to moderate dense and sparse forest changes were greater from 1975 to 1990 than the other two transitional periods (1990 to 2005 and 2005 to 2020). However, very few areas of dense forest were developed from the moderate dense, sparse forest and other types of land cover. The study found that the highest percentages of dense forests were developed from 1990 to 2005 by replacing moderate dense to dense (5.65%) and sparse to dense forest (3.61%). The barren areas were increased by converting moderate dense forest to the barren land and sparse forest to barren land from 1975 to 2020. But, barren lands were decreased in areas by dense forest from 1975 to 1990. A significant amount of barren, sparse, dense, and moderate dense forests areas turned into water bodies from 1975 to 2020, where very few areas gained from water (Figure 6).

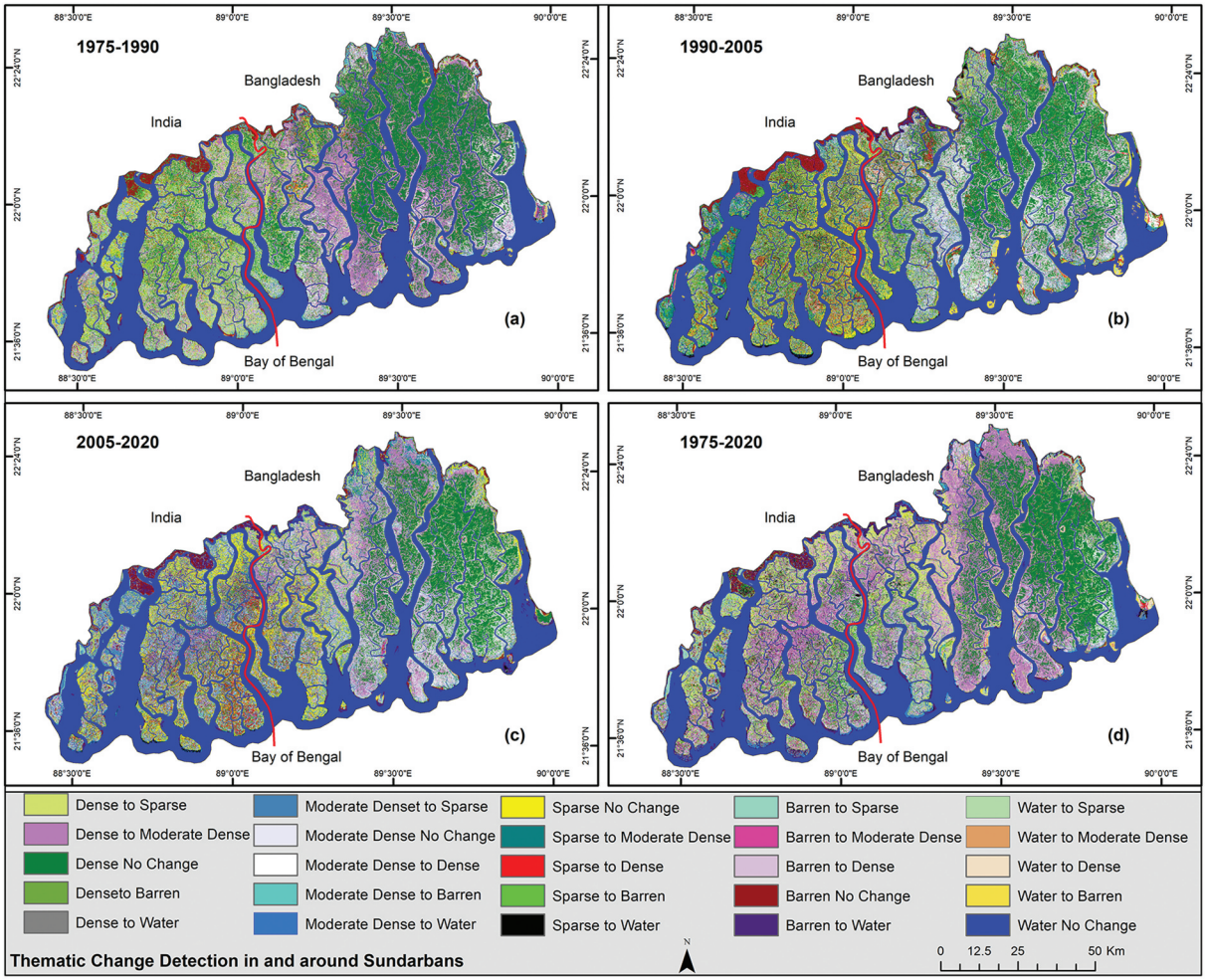

Figure 6. Thematic Changes in and around Sundarbans from 1975 to 2020.

Positive, negative and unchanged in and around Sundarbans

The findings of our result showed that the no-change[1] areas were greater than negative[2] and positive change[3] areas from 1975 to 2020. But, most of the no-change areas included water bodies. The no-change areas were more numerous for the period from 1990 to 2005, and these areas were located in the eastern part of Sundarbans (Figure 7). Maximum positive changes occurred from 1975 to 1990 than the other two periods (e.g. 1990 to 2005 and 2005 to 2020), which were found in the eastern part of the forest. The negative change areas were highest 2005 to 2020 (Figure 8) compared to other periods.

Discussion

Accuracy assessment

The overall accuracy and kappa coefficient of this study found are higher than the obtained by Mandal and Hosaka (2020), Nandy and Kushwaha (2011), and Giri et al. (2007). It is considered as a significantly high level of agreement with validation data (Landis & Koch, 1977; Rwanga & Ndambuki, 2017). The producer's (PA) and user's (UA) accuracy of our study were higher for water than for sparse and moderate forest. This is likely due to the spectral similarity between the sparse and moderate forest, which both have photosynthetic material with background of soil or other which mix the spectral response. Moreover, the Landsat-8 OLI-TIRS sensor (2020) classified images had higher overall accuracy and kappa values compared to TM (2005), MSS (1990), and MSS (1975) (Table 2). The reason behind that the training samples were not closely matched with image date, although we used Google Earth high-resolution images as reference data for the years 2020, 2005 and 1990, and historical land use maps (e.g. toposheet map) for the year 1975 (Islam et al., 2019; Kumar et al., 2021).

[1]No change indicates the stable areas where no alternation among dense forest, moderate dense forest, sparse forest, barren land and water bodies.
[2]Negative change indicates the decrease of dense forest, moderate dense forest, sparse forest, barren land and water bodies.
[3]Positive change indicates the increase of dense forest, moderate dense forest, sparse forest, barren land and water bodies.

Table 4. Analysis thematic changes of Sundarbans (1975–2020).

	1975–1990		1990–2005		2005–2020		1975–2020	
Change classes	km^2	%	km^2	%	km^2	%	km^2	%
Dense to sparse	848	8.48	398	3.97	460	4.59	1041	10.41
Dense to moderate dense	1331	13.3	352	3.51	847	8.45	1563	15.62
Dense no change	2275	22.74	1830	18.24	1332	13.28	1625	16.24
Dense to barren	38	0.38	29	0.29	42	0.42	51	0.51
Dense to water	31	0.31	44	0.44	137	1.37	245	2.45
Moderate dense to sparse	275	2.75	454	4.52	635	6.33	310	3.1
Moderate dense no change	358	3.57	765	7.63	702	7	242	2.42
Moderate dense to dense	120	1.2	567	5.65	294	2.93	128	1.28
Moderate dense to barren	36	0.36	7	0.07	30	0.3	22	0.22
Moderate dense to water	19	0.19	23	0.23	73	0.73	106	1.06
Sparse no change	220	2.2	481	4.79	559	5.57	154	1.54
Sparse to moderate dense	55	0.55	574	5.72	493	4.91	125	1.25
Sparse to dense	120	1.2	363	3.61	220	2.2	44	0.44
Sparse to barren	82	0.82	142	1.42	20	0.2	38	0.38
Sparse to water	53	0.53	177	1.76	71	0.7	169	1.69
Barren to sparse	349	3.49	15	0.15	89	0.88	251	2.51
Barren to moderate dense	62	0.62	32	0.32	50	0.5	162	1.62
Barren to dense	124	1.24	21	0.21	16	0.16	52	0.52
Barren no change	241	2.4	249	2.48	136	1.36	120	1.2
Barren to water	222	2.22	101	1.01	229	2.28	413	4.13
Water to sparse	37	0.37	15	0.15	78	0.77	59	0.59
Water to moderate dense	8	0.08	11	0.11	33	0.33	29	0.29
Water to dense	8	0.08	37	0.36	5	0.05	15	0.15
Water to barren	19	0.19	94	0.94	18	0.18	16	0.16
Water no change	3072	30.7	3252	32.41	3461	34.5	3024	30.23

Land use land cover, thematic change, and positive, negative and unchanged

The dense forest cover was highest in 1975 compared to other periods (e.g. 1990, 2005, and 2020). However, the study found that the dense forest area reduced from 1975 to 1990 and 2005 to 2020, and it increased from 1990 and 2005. In the overall study timespan (1975 to 2020), the dense area declined with an annual rate of 1.3%. Giri et al. (2007) reported that the Sundarbans mangrove forest area decreased by 1.2% from 1970 to 2000. Our thematic change study showed that the changing patterns of the dense and moderate forests were opposite from 1975 to 2020 (Figure 9); when the dense forest decreased, the moderate dense forest increased with the same trend. A similar opposite trend was also found between the sparse and barren lands. The findings of these thematic changes suggest that the Sundarbans dense forest deceased by converting to moderate dense and sparse forest, whereas most of the sparse turned into barren land. However, the degradation rate is increasing due to anthropogenic activities, natural, and climate change factors. Anthropogenic activities include overexploitation of resources (e.g. honey, fuelwood, thatching materials, fish, crab, medicinal plants, etc.), agricultural expansion (e.g. shrimp farming and paddy cultivation), and industrialization (e.g., power plant, dam construction, port, and shipyard) (Giri et al., 2007; Ghosh et al., 2015; Iftekhar & Islam, 2004; Islam, 2010; Kumar et al., 2021; Rahman et al., 2010; Thakur et al., 2021). Natural factors comprise tropical cyclones, storm surges, salinity intrusion, siltation, and pest and diseases (Ghosh et al., 2015; Islam & Gnauck, 2008; Kumar et al., 2021; Mandal & Hosaka, 2020; Neogi et al., 2017; Quader et al., 2017; Rahman et al., 2015). The major climate change reason is sea level rise for the Sundarbans (Ghosh et al., 2015; Kumar et al., 2021; Loucks et al., 2010; Payo et al., 2016; Quader et al., 2017).

Anthropogenic activities

Anthropogenic activities are one of the major causes of the degradation of Sundarbans (Das & Datta, 2016). For instance, approximately 3.5 million Bangladeshi and 4 million Indian people are directly or indirectly dependent on Sundarbans for livelihood and socio-economic well-being (Giri et al., 2007; Kibria et al., 2018; Ortolano et al., 2016; Roy et al., 2013). However, the number of forest-dependent people is still increasing in Sundarbans areas, leading to rising overexploitation of resources to meet the demand (Ghosh et al., 2015; Nishat et al., 2019). Rahman et al. (2010) also reported that the areas of Sundarbans and its biodiversity is disappearing quickly due to illegal felling, encroachment, and poaching of wildlife.

Our study found that the moderate and sparse forests were highest than the dense forest in 2020. The highest amount of barren lands were fund for 1975, and then it reduced in 2020. However, most of the barren land areas are located near the border between forest and human habitat (Figure 4),

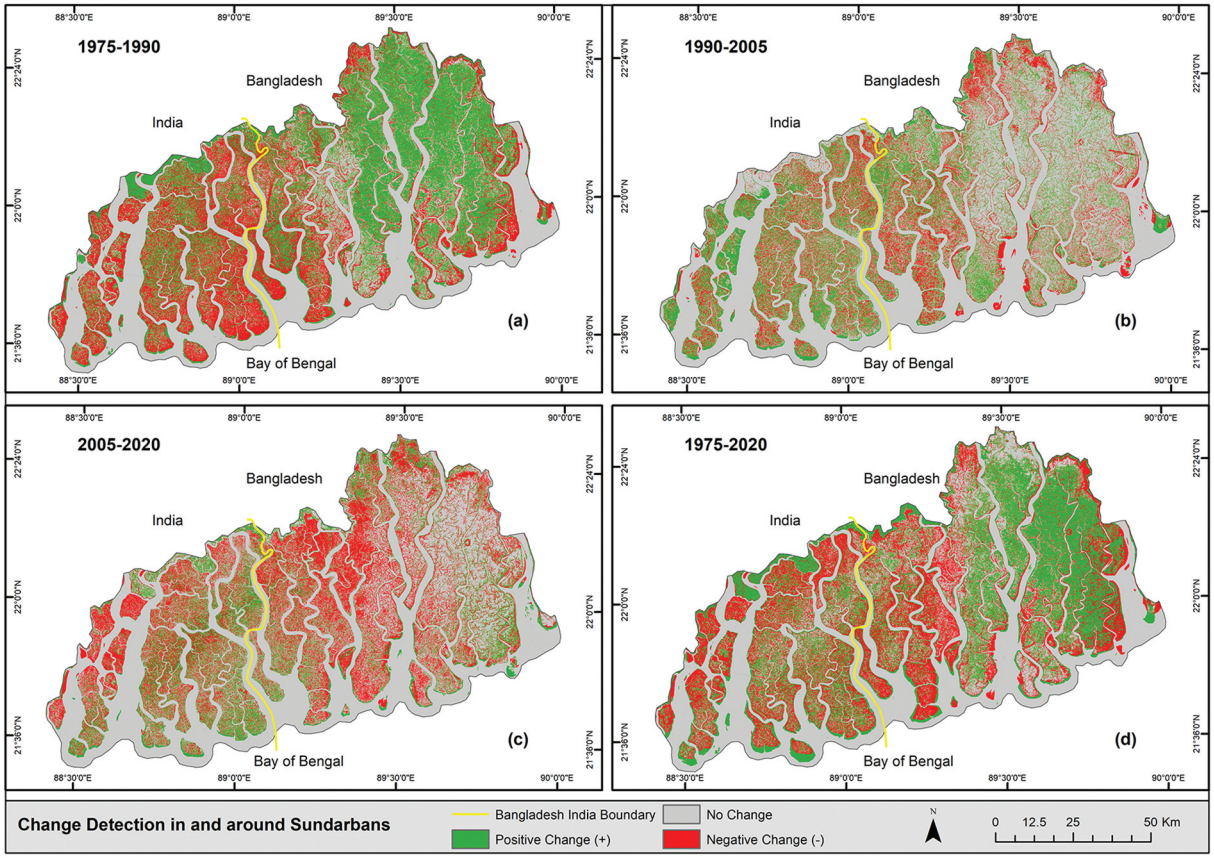

Figure 7. Areas with forest change of Sundarbans from 1975 to 2020.

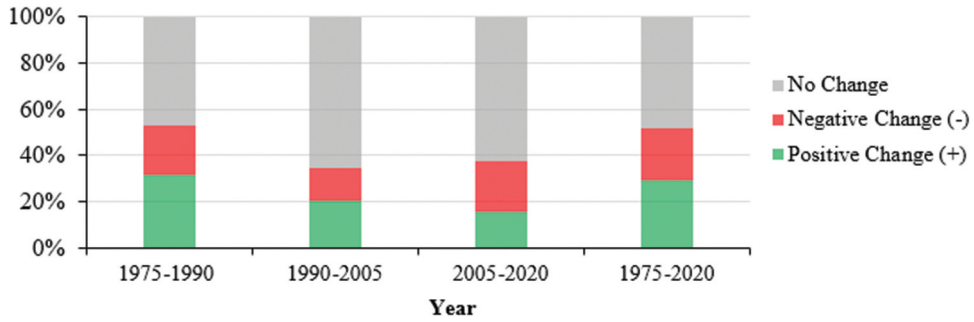

Figure 8. Forest change in Sundarbans from 1975 to 2020.

indicating human-induced degradations. Kumar et al. (2021) reported that the settlement and agricultural expansion reduce the forest covered area adjacent to Sundarbans' boundary. According to the Zoological Society of London (2012), the agricultural activities had destroyed around 24,730 ha of Sundarbans mangroves from 1975–2010, where only shrimp cultivation destroyed 7,550 ha (Neogi et al., 2017). Aziz and Paul (2015) also reported that 110 km^2 (11000 ha) Sundarbans reduced from 1970 to 2000. Our LULC map showed that the sparse forest and barren land areas were highest in the Indian part of Sundarbans than in Bangladesh (Figure 4). Similar results were found by Thakur et al. (2021) and Quader et al. (2017). Paul et al. (2017) reported that the southwestern part of Indian Sundarbans is degraded mainly for human uses of mangrove resources, fishery development, hypersalinity, siltation, cyclonic storm effects, and land erosion.

Construction of dam and other industrial development are continuing around the Sundarbans to grow up country's economy which led to increasing the reasons of forest degradations. Islam and Gnauck (2008) reported that the Ganges waterway decreased freshwater discharge from 3700 m^3s^{-1} in 1962 to 364 m^3s^{-1} in 2006 due to the construction of the Farakka Barrage in 1975, resulting in increasing salinity level of the Sundarbans and decreasing forest

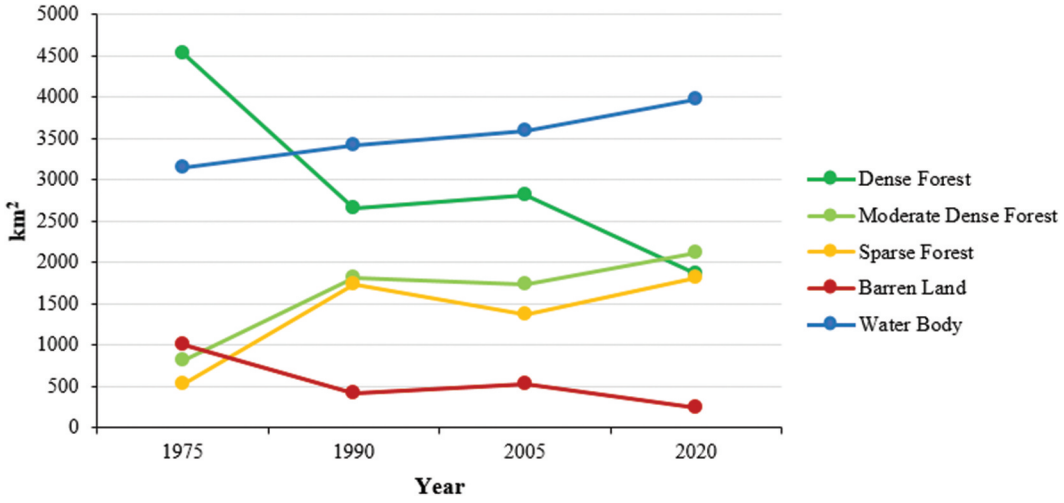

Figure 9. Changing pattern of different LULC of Sundarbans from 1975 to 2020.

cover. In our study the forest density was always (1975–2020) higher in the eastern part of Sundarbans compared to other areas (Figure 4). Because salinity decreases from west to east (Gopal & Chauhan, 2006) and dominates by less salinity lover *Heritiera fomes* tree (Aziz & Paul, 2015). Rahman et al. (2015) reported that, *Heritiera fomes* dominated forest types store more ecosystem carbon than other vegetation types. However, the *Heritiera fomes* dominated forest stands (eastern part) are also decreasing due to increasing soil salinity. Mukhopadhyaya et al. (2015) and Aziz and Paul (2015) reported that about 32% of Bangladesh Sundarbans were covered by only *Heritiera fomes* in 1959 that reduced to 21% in 1983 and 17% in 2015. In addition, Bangladesh and Indian governments recently agreed to build a coal-fed thermal power plant in Rampal 14 km north of the Sundarbans is an additional reason for Sundarbans degradation.

Natural factors

Cyclone disturbances can cause significant damage to forest structures (Everham & Brokaw, 1996) and forested landscapes (Foster & Boose, 1992). Sundarbans is on an average 150 km long (east to west) and 75 km wide (north to south), which acts as a natural barrier that protects the coastal people and their properties from cyclonic storms, tidal surges, and coastal soil erosions. Every year, the tropical cyclones with different intensities across the coastal areas of Bangladesh (Alam & Collins, 2010; Mallick et al., 2017), most of the landfall starts from Sundarbans. Moreover, Sundarbans face severe cyclonic storms and disturbances every 7–12 years (Mandal & Hosaka, 2020). In our map, we showed the cyclone tract that happened just before the study periods (Figure 10). The findings of our study revealed that tropical cyclones damaged Sundarbans massively from 1975 to 2020. The intensity of cyclone disturbances depends on wind speed, distance from the cyclone's eye, precipitation, and so on (Mandal & Hosaka, 2020). The maximum wind speed of our reported four cyclonic events were 80 km h^{-1} (1974), 102 km h^{-1} (1989), 101 km h^{-1} (2005), and 195 km h^{-1} (2019) (Mandal & Hosaka, 2020; Quader et al., 2017). Among four cyclonic events, the cyclone Bulbul (2019) had high wind speed and damaged the Sundarbans significantly. Samanta et al. (2021) estimated that, 14.6% (303.6 km^2) and 45.8% (950.7 km^2) of Indian Sundarbans areas suffered high and low loss, respectively, due to the cyclone Bulbul. Similarly, Bangladesh Sundarbans seems affected significantly after the cyclonic storms Bulbul. Another two severe cyclones, namely Sidr (2007) and Aila (2009), damaged the Sundarbans vastly. For instance, cyclone Sidr affected the Sundarbans most severely, where 24% of forest was destroyed by trunk breakage, uprooting, substrate loss, and local scour around the trees (Mandal & Hosaka, 2020). Recently, super-cyclonic storm Amphan (2020) attacked the western part of Sundarbans caused considerable damages to the forest biodiversity. Neogi et al. (2017) reported that the cyclonic storms are increased by 26% from 1881 to 2001 towards the Sundarbans coastal area, and the degree of the tropical cyclonic impacts is expected to extremely high in the next few years (Alam & Dominey-Howes, 2015; Moon et al., 2019; Ranson et al., 2014; Varotsos et al., 2015; Walsh et al., 2016). Therefore, cyclonic storms are the major causes for the degradation of Sundarbans mangrove. In addition to this, the landmass of Sundarbans (i.e. offshore islands and sea-facing coastlines) is reducing due to tidal surges. Kanan

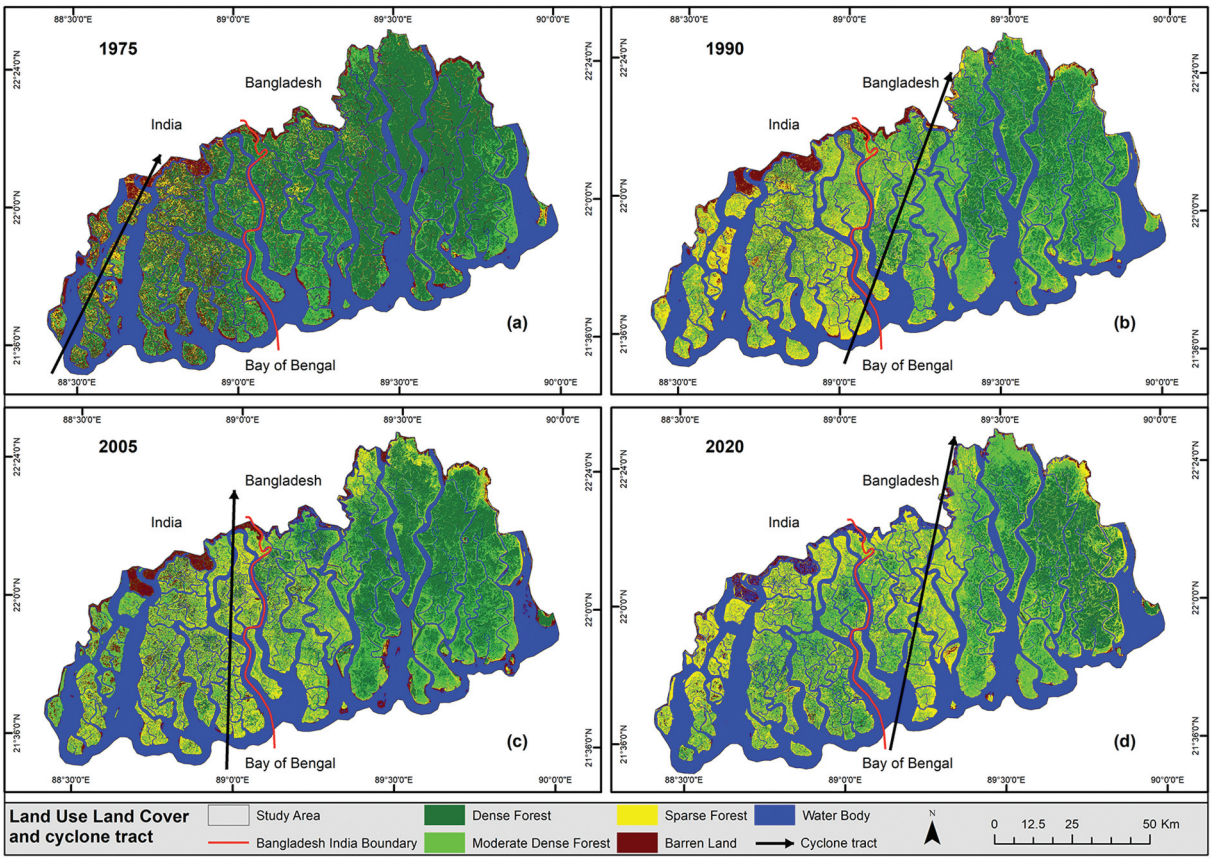

Figure 10. LULC and cyclone tract from 1975 to 2020. Cyclone track of August 1974 (a), November 1989 (b) November 2002 (c) and November 2019 (d).

et al. (2021) studied that the net erosion of Sundarbans was 821 km^2 for the last 45 years (1975 to 2020).

Climate change factors

Sundarbans is an innocent victim of accelerating global warming, and sea level rise is considered the most significant climate change-related threat to Sundarbans (Loucks et al., 2010; Quader et al., 2017). In our study, the area water bodies of Sundarbans increased gradually from 1975 to 2020 (Figure 9). Quader et al. (2017) studied that the water bodies and sea level increased gradually from 1977 to 2010, which might indicate sea level reduces some areas of Sundarbans. Nishat et al. (2019) reported that the sea level rise in the Sundarbans is +3.90 ± 0.46 mm/year, and 75% of mangrove area will inundate if sea-level rise will grow up to 0.45 m (Jabir et al., 2021) . Sea level rise increases both the surface water salinity and soil salinity through the saline water intrusion into the groundwater (Bhuyian & Dushmanta, 2011) and reduces the forest's diversity and density. The water and soil salinity level of the north-eastern Bangladesh Sundarbans is less than other parts of the forest (Aziz & Paul, 2015; Gopal & Chauhan, 2006); therefore, we found a higher density for the north-eastern part (Figure 4). Generally, high-density forest sinks more carbon is significant to reduce greenhouse gas emissions to the atmosphere. Donato et al. (2011) reported that the carbon sequestration rate of mangrove forests is, on average, four times higher than other tropical forests. Therefore, scientific management of Sundarbans might increase the total ecosystem carbon stock than it already has stored.

Challenges and uncertainties for mapping and assessing

First, LULC long-term study of Sundarbans is challenging, because multiple scenes from multiple sensors are required to cover Sundarbans for the whole time period (Islam et al., 2019; Roy & Inamdar, 2019). For this reason, the collection of cloud-free multiple images for a common date and sensor is not possible. Therefore, our study tried to keep the nearest date to collect multiple images maintaining the same spectral signature. Moreover, we followed the standard method for reducing radiometric, atmospheric, and mosaicking effects.

Second, the tide inundates the Sundarbans twice a day (Barlow et al., 2011), ranging between 1 m to 1.5 m. The tidal range (e.g. high, low, and mid-tide)

influences the mangrove LULC mapping using satellite data (Zhang et al., 2015). Therefore, we analysed station-based hourly tidal data of Sundarbans (1977 to 2020) to understand the sensitivity of tidal variations of the images used in the LULC classification. The maximum tidal difference among these collected images was around half a meter. The less tidal variation might be that the Landsat satellites flew and captured the images of Sundarbans regions when it was at a mid-tide level at that time (9:30 am to 10:30 am) (Table 1). Thus, no significant changes in exposure or coverage to mudflat and inter-tidal regions of the images used in the study, and the best condition for LULC mapping of Sundarbans mangroves.

Third, during LULC classification, we observed that the water color was different near the shoreline areas than the deep river basins of Sundarbans and produced slightly different spectral variations. The deep and shallow water color is different due to the sedimentation, water deepness, and tidal effect (Islam et al., 2019). In this situation, we selected a large number of water body sites as a training sample for accurate classification. Therefore, mangrove LULC classification needs more attention to overcome the sedimentation, water deepness and tidal effect.

Fourth, we verified control points over the classified images using Google Earth historical images except the year 1975. In this situation, we verified images using previous literature, expert-based information (Quader et al., 2017) and historical toposheet map of Sundarbans.

Finally, Landsat data are effective for mapping and assessing spatio-temporal changes of Sundarbans. However, it needs to follow a proper methodology to obtain higher accuracy. For instance, selecting training samples by careful inquiry of homogeneous pixels increases the maximum likelihood classification accuracy. In addition, verification with more control points is important for accurate measuring of LULC change over time.

Conclusion

The present study used multiple Landsat scenes and sensors to estimate LULC, thematic and net changes of the entire Sundarbans mangrove. The Landsat images were processed using an appropriate methodological approach to ensure accurate mapping and estimation. As a result, we found higher accuracy than the previous study of Sundarbans. The overall accuracy and kappa coefficient ranges were from 84.8% to 90.0% and 0.81 to 0.87, respectively, suitable for monitoring mangrove forests. These accuracy metrics were higher for Landsat-8 (OLI-TIRS) compared to Landsat-2 (MSS) and Landsat-5 (TM).

The study found that in the overall study timespan from 1975 to 2020, the dense forest cover of Sundarbans decreased by giving an annual rate of 1.3%; however, the decreasing rate was unstable. The dense forest area decreased from 1975 to 1990 and 2005 to 2020, where it increased from 1990 to 2005. The dense forest cover decreased by altering to moderate dense and sparse forest, whereas most sparse areas turned barren land. However, very few dense and moderate dense forest areas were developed from the sparse forest and barren lands. Most of the barren lands were found near the borderline between forest and human settlement, and these two types of land cover were higher for the Indian part of Sundarbans than Bangladesh. Human-induced activities and cyclonic storms were the significant causes for the degradation of Sundarbans.

However, the government of Bangladesh and India take the initiative to protect the Sundarbans by updating their management policies, but implementation is quite challenging or incomplete (Ghosh et al., 2015; Mahmood et al., 2021). Therefore, governments need to collaborate with policymakers, ecologists, environmentalists, activists, and local people to improve management strategies. The coastal belt plantation and control access of forest-dependent people by generating alternative income sources could effectively conserve Sundarbans and its biodiversity. Using remote sensing multitemporal data, like in this research, helps support sustainable forest management and planning, particularly in scenarios like the Sundarbans, contributing to the achievement of some UN-SDGs.

Author contributions

AHK performed literature review, experimental design, data analysis and interpretation, manuscript writing and editing. FP designed the research, contributed to writing the text, supervised the study, and reviewed the manuscript. MM provided insight regarding interpretation and edition of writing of this research.

Disclosure statement

No potential conflict of interest was reported by the authors.

Funding

This work was supported by the University of Padova and CARIPARO (Fondazione Cassa di Risparmio di Padova e Rovigo).

ORCID

Kanan Akbar Hossain http://orcid.org/0000-0002-5943-3615
Mauro Masiero http://orcid.org/0000-0001-5660-4362
Francesco Pirotti http://orcid.org/0000-0002-4796-6406

Data availability statement

Landsat data used in this work is openly available. The original images used and the resulting classified rasters are available at the link: https://figshare.com/s/a2435b4039c093cd793f or 10.6084/m9.figshare.19089977.

References

Alam, E., & Collins, A. E. (2010). Cyclone disaster vulnerability and response experiences in coastal Bangladesh. *Disasters*, *34*(4), 931–954. https://doi.org/10.1111/j.1467-7717.2010.01176.x

Alam, E., & Dominey-Howes, D. (2015). A new catalogue of tropical cyclones of the northern Bay of Bengal and the distribution and effects of selected landfalling events in Bangladesh. *International Journal of Climatology*, *35*(6), 801–835. https://doi.org/10.1002/joc.4035

Aziz, A., & Paul, A. R. (2015). Bangladesh Sundarbans: Present status of the environment and Biota. *Diversity*, *7*(3), 242–269. https://doi.org/10.3390/d7030242

Barbier, E. B. (2007). Valuing ecosystem services as productive inputs. *Economic Policy*, *22*(49), 177–229. https://doi.org/10.1111/j.1468-0327.2007.00174.x

Barlow, A. C. D., Smith, J. L. D., Ahmad, I. U., Hossain, A. N. M., Rahman, M., & Howlader, A. (2011). Female tiger *Panthera Tigris* home range size in the Bangladesh Sundarbans: The value of this mangrove ecosystem for the species-conservation. *Oryx*, *45*(1), 125–128 https:/doi.org/10.1017/S0030605310001456

Bera, S., & Chatterjee, N. D. (2019). Mapping and monitoring of land use dynamics with their change hotspot in North 24-Parganas district, India: A geospatial- and statistical-based approach. *Modeling Earth Systems and Environment*, *5*(4), 1529–1551. https://doi.org/10.1007/s40808-019-00601-2

Bhuyian, M. J. A. N., & Dushmanta, D. (2011). Assessing impacts of sea level rise on river salinity in the Gorai river network, Bangladesh. *Estuarine, Coastal and Shelf Science*, *96*(1), 219–227. https://doi.org/10.1016/j.ecss.2011.11.005

Billah, M. M., Rahman, M. M., Abedin, J., & Akter, H. (2021). Land cover change and its impact on human–elephant conflict: A case from Fashiakhali forest reserve in Bangladesh. *SN Applied Sciences*, *3*(6), 649. https://doi.org/10.1007/s42452-021-04625-1

Chanda, A., Mukhopadhyay, A., Ghosh, T., Akhand, A., Mondal, P., Ghosh, S., Hazra, S., Wolf, J., Lázár, A. N., Rahman, M. M., Salehin, M., Chowdhury, S. M., & Hazra, S. (2016). Blue carbon stock of the Bangladesh Sundarban Mangroves: What could be the scenario after a century? *Wetlands*, *36*(6), 1033–1045. https://doi.org/10.1007/s13157-016-0819-7

Chen, C. F., Son, N. T., Chang, N. B., Chen, C. R., Chang, L. Y., Valdez, M., Aceituno, J. L., Thompson, C., & Aceituno, J. (2013). Multi-decadal mangrove forest change detection and prediction in Honduras, Central America, with Landsat imagery and a Markov chain model. *Remote Sensing*, *5*(12), 6408–6426. https://doi.org/10.3390/rs5126408

Chirici, G. (2020). Earth observation for the implementation of sustainable development goals: The role of the. *European Journal of Remote Sensing. European Journal of Remote Sensing*, *53*(1), i–ii. https://doi.org/10.1080/22797254.2020.1756119

Congalton, R. G. (1991). A review of assessing the accuracy of classifications of remotely sensed data. *Remote Sensing of Environment*, *37*(1), 35–46. https://doi.org/10.1016/0034-4257(91)90048-B

Dahdouh-Guebas, F., Hiel, E. V., Chan, J. C. W., Jayatissa, L. P., & Koedam, N. (2004). Qualitative distinction of congeneric and introgressive mangrove species in mixed patchy forest assemblages using high spatial resolution remotely sensed imagery (IKONOS). *Systematics and Biodiversity*, *2*(2), 113–119. https://doi.org/10.1017/S1477200004001422

Das, G. K., & Datta, S. (2016). Man-Made environmental degradation at Sunderbans. *Reason-A Technical Journal*, *13*, 89. https://doi.org/10.21843/reas/2014/89-106/108127

Datta, D., & Deb, S. (2012). Analysis of coastal land use/land cover changes in the Indian Sundarbans using remotely sensed data. *Geo-spatial Information Science*, *15*(4), 241–250 https://doi.org/10.1080/10095020.2012.714104

Donato, D. C., Kauffman, J. B., Murdiyarso, D., Kurnianto, S., Stidham, M., & Kanninen, M. (2011). Mangroves among the most carbon-rich forests in the tropics. *Nature Geoscience*, *4*(5), 293–297.https://doi.org/10.1038/ngeo1123

Emch, M., & Peterson, M. (2006). Mangrove forest cover change in the Bangladesh Sundarbans from 1989-2000: A Remote Sensing Approach. *Geocarto International*, *21*(1), 5–12 https://doi.org/10.1080/10106040608542368

Everham, E. M., & Brokaw, N. V. (1996). Forest damage and recovery from catastrophic wind. *Botanical Review*, *62*(2), 113–185. https://doi.org/10.1007/BF02857920

FAO. 2010. Global forest resources assessment 2010: Main report. Food and Agriculture Organization of the United Nations. Forestry Paper. 978-92-5-106654-6

Foster, D. R., & Boose, E. R. (1992). Patterns of forest damage resulting from catastrophic wind in central New England, USA. *Journal of Ecology*, *80*(1), 79–98. https://doi.org/10.2307/2261065

Ghosh, A., Schmidt, S., Fickert, T., & Nüsser, M. (2015). The Indian Sundarban Mangrove forests: History, utilization, conservation strategies and local perception. *Diversity*, *7*(2), 149–169. https://doi.org/10.3390/d7020149

Ghosh, M. K., Kumar, L., & Roy, C. (2016). Mapping long-term changes in Mangrove species composition and distribution in the Sundarbans. *Forests*, *7*(12), 305. https://doi.org/10.3390/f7120305

Giri, C., Pengra, B., Zhu, Z., Singh, A., & Tieszen, L. L. (2007). Monitoring mangrove forest dynamics of the Sundarbans in Bangladesh and India using multi-temporal satellite data from 1973 to 2000. *Estuarine, Coastal and Shelf Science*, *73*(1–2), 91–100. https://doi.org/10.1016/j.ecss.2006.12.019

Giri, C., & Muhlhausen, J. (2008). Mangrove forest distributions and dynamics in Madagascar (1975-2005). *Sensors (Basel)*, *8*(4), 2104–2117 https://doi.org/10.3390/s8042104

Giri, C., Ochieng, E., Tieszen, L. L., Zhu, Z., Singh, A., Loveland, T., Masek, J., & Duke, N. (2010). Status and distribution of mangrove forests of the world using earth observation satellite data. *Global Ecology and Biogeography*, *20*(1), 154–159. https://doi.org/10.1111/j.1466-8238.2010.00584.x

Giri, S., Anirban, M., Sugata, H., Sandip, M., Deborupa, R., Subhajit, G., Tuhin, G., & Debasish, M. (2014). A study on abundance and distribution of mangrove species in Indian Sundarban using remote sensing technique. *Journal of Coastal Conservation*, *18*(4), 359–367. http://dx.doi.org/10.1007/s11852-014-0322-3

Gopal, B., & Chauhan, M. (2006). Biodiversity and its conservation in the sundarban mangrove ecosystem. *Aquatic Sciences*, *68*(3), 338–354. https://doi.org/10.1007/s00027-006-0868-8

Hasan, M. E., Nath, B., Sarker, A. H. M. R., Wang, Z., Zhang, L., Yang, X., Nobi, M. N., Røskaft, E., Chivers, D. J., & Suza, M. (2020). Applying multi-temporal landsat satellite data and Markov-cellular automata to predict forest cover change and forest degradation of Sundarban Reserve Forest, Bangladesh. *Forests*, *11*(9), 1–35. https://doi.org/10.3390/f11091016

Hassan, M. M. (2017). Monitoring land use/land cover change, urban growth dynamics and landscape pattern analysis in five fastest urbanized cities in Bangladesh. *Remote Sensing Applications: Society and Environment*, *7*, 69–83. https://doi.org/10.1016/j.rsase.2017.07.001

Iftekhar, M. S., & Islam, M. R. (2004). Degeneration of Bangladesh's Sundarbans mangroves: A management issue. *International Forestry Review*, *6*(2), 123–135. https://doi.org/10.1505/ifor.6.2.123.38390

Ishtiaque, A., & Chhetri, N. (2016). Competing policies to protect mangrove forest: A case from Bangladesh. *Environmental Development*, *19*, 75–83. https://doi.org/10.1016/j.envdev.2016.06.006

Islam, S. N., & Gnauck, A. (2008). Mangrove wetland ecosystems in Ganges-Brahmaputra delta in Bangladesh. *Frontiers of Earth Science in China*, *2*(4), 439–448. https://doi.org/10.1007/s11707-008-0049-2

Islam, D. K. M. N. (2010). *Integrated Protected Area Co-Management (IPAC) - A Study of the Principal Marketed Value Chains Derived from the Sundarbans Reserved Forest*. USAID.

Islam, M. M., Borgqvist, H., & Kumar, L. (2019). Monitoring Mangrove forest landcover changes in the coastline of Bangladesh from 1976 to 2015. *Geocarto International*, *34*(13), 1458–1476. https://doi.org/10.1080/10106049.2018.1489423

Jat, M. K., Garg, P. K., & Khare, D. (2017). Modelling of urban growth using spatial analysis techniques: A case study of Ajmer City (India). *International Journal of Remote Sensing*, *29*(2), 543–567. https://doi.org/10.1080/01431160701280983

Jones, T. G., Glass, L., Gandhi, S., Ravaoarinorotsihoarana, L., Carro, A., Benson, L., Ratsimba, H. R., Giri, C., Randriamanatena, D., & Cripps, G. (2016). Madagascar's mangroves: Quantifying nation-wide and ecosystem specific dynamics, and detailed contemporary mapping of distinct ecosystems. *Remote Sensing*, *8*(2), 106. https://doi.org/10.3390/rs8020106

Kanan, A. H., Pirotti, F., & Masiero, M. (2021). Analysing change dynamics of land cover, erosion and accretion of world's largest mangrove forest (Sundarbans) using remotely sensed data. *40 th EARSeL Symposium*, 7-10 June, 2021, University of Warsaw, Poland.

Kanniah, K. D., Sheikhi, A., Cracknell, A. P., Goh, H. C., Tan, K. P., Ho, C. S., & Rasli, F. N. (2015). Satellite images for monitoring mangrove cover changes in a fast-growing economic region in southern Peninsular Malaysia. *Remote Sensing*, *7*(11), 14360–14385 https://doi.org/10.3390/rs71114360

Kaufman, Y. J., Wald, A. E., Remer, L. A., Gao, B. C., Li, R. R., & Flynn, L. (1997). The MODIS 2.1-μm channel-correlation with visible reflectance for use in remote sensing of aerosol. *IEEE Transactions on Geoscience and Remote Sensing*, *35*(5), 1286–1298. https://doi.org/10.1109/36.628795

Kibria, A. S. M. G., Costanza, R., Groves, C., & Behie, A. M. (2018). The interactions between livelihood capitals and access of local communities to the forest provisioning services of the Sundarbans Mangrove forest, Bangladesh. *Ecosystem Services*, *32*(A), 41–49. https://doi.org/10.1016/j.ecoser.2018.05.003

Knorn, J., Rabe, A., Radeloff, V. C., Kuemmerle, T., Kozak, J., & Hostert, P. (2009). Land cover mapping of large areas using chain classification of neighboring Landsat satellite images. *Remote Sensing of Environment*, *113*(5), 957–964. https://doi.org/10.1016/j.rse.2009.01.010

Kumar, M., Mondal, I., & Pham, Q. B. (2021). Monitoring forest landcover changes in the Eastern Sundarban of Bangladesh from 1989 to 2019. *Acta Geophysica*, *69*(2), 561–577. https://doi.org/10.1007/s11600-021-00551-3

Landis, J. R., & Koch, G. G. (1977). The measurement of observer agreement for categorical data. *Biometrics*, *33*(1), 159–174. https://doi.org/10.2307/2529310

LaRocque, A., Phiri, C., Leblon, B., Pirotti, F., Connor, K., & Hanson, A. (2020). Wetland mapping with landsat 8 OLI, sentinel-1, ALOS-1 PALSAR, and LiDAR data in Southern New Brunswick, Canada. *Remote Sensing*, *12*(13), 2095. https://doi.org/10.3390/rs12132095

Li, C., Wang, J., Wang, L., Hu, L., & Gong, P. (2014). Comparison of classification algorithms and training sample sizes in urban land classification with Landsat thematic mapper imagery. *Remote Sensing*, *6*(2), 964–983. https://doi.org/10.3390/rs6020964

Loucks, C., Mayer, S. B., Hossain, M. A. A., Barlow, A., & Chowdhury, R. M. (2010). Sea level rise and tigers: Predicted impacts to Bangladesh's Sundarbans mangroves: A letter. *Climate Change*, *98*(1–2), 291–298. https://doi.org/10.1007/s10584-009-9761-5

Lu, D., & Weng, Q. (2007). A survey of image classification methods and techniques for improving classification performance. *International Journal of Remote Sensing*, *28*(5), 823–870. https://doi.org/10.1080/01431160600746456

Mahmood, H., Ahmed, M., Islam, T., Uddin, M. Z., Ahmed, Z. U., & Saha, C. (2021). Paradigm shift in the management of the Sundarbans mangrove forest of Bangladesh: Issues and challenges. *Trees, Forests and People*, *5*(100094), 1–14. https://doi.org/10.1016/j.tfp.2021.100094

Malik, A., Mertz, O., & Fensholt, R. (2017). Mangrove forest decline: Consequences for livelihoods and environment in South Sulawesi. *Regional Environmental Change*, *17*(1), 157–169. https://doi.org/10.1007/s10113-016-0989-0

Mallick, B., Ahmed, B., & Vogt, J. (2017). Living with the risks of cyclone disasters in the south-western coastal region of Bangladesh. *Environments*, *4*(1), 13. https://doi.org/10.3390/environments4010013

Mandal, M. H. S., & Hosaka, T. (2020). Assessing cyclone disturbances (1988–2016) in the Sundarbans mangrove forests using landsat and google earth engine. *Natural Hazards*, *102*(1), 133–150. https://doi.org/10.1007/s11069-020-03914-z

Matthew, M. W., Adler-Golden, S. M., Berk, A., Richtsmeier, S. C., Levine, R. Y., Bernstein, L. S., Acharya, P. K., Anderson, G. P., Felde, G. W., Hoke, M. P., Ratkowski, A., Burke, H. H., Kaiser, R. D., & Miller, D. P. (2000). Status of atmospheric correction using a MODTRAN4-based Algorithm. *SPIE Proceedings, Algorithms for Multispectral, Hyperspectral, and Ultraspectral Imagery*, 4049, 199–207.

Moon, I. J., Kim, S. H., & Chan, J. C. (2019). Climate change and tropical cyclone trend. *Nature*, *570* (7759), E3–E5 https://doi.org/10.1038/s41586-019-1222-3

Mukhopadhyaya, A., Mondala, P., Barika, J., Chowdhuryb, S. M., Ghosha, & Hazraa, S. (2015). Changes in mangrove species assemblages and future prediction of the Bangladesh Sundarbans using Markov Chain model and Cellular Automata. *Environmental Science. Processes & Impacts*, *17*(6), 1111–1117. https://doi.org/10.1039/c4em00611a

Myeong, S., Nowak, D. J., & Duggin, M. J. (2006). A temporal analysis of urban forest carbon storage using remote sensing. *Remote Sensing of Environment*, *101*(2), 277–282. https://doi.org/10.1016/j.rse.2005.12.001

Nandy, S., & Kushwaha, S. P. S. (2011). Study on the utility of IRS 1D LISS-III data and the classification techniques for mapping of Sundarban mangroves. *Journal of Coastal Conservation*, *15*(1), 123–137. https://doi.org/10.1007/s11852-010-0126-z

Neogi, S. B., Dey, M., Kabir, S. L., Masum, S. J. H., Kopprio, G., Yamasaki, S., & Lara, R. (2017). Sundarban mangroves: Diversity, ecosystem services and climate change impacts. *Asian Journal of Medical and Biological Research*, *2*(4), 488–507. https://doi.org/10.3329/ajmbr.v2i4.30988

Nishat, B., Rahman, A. J. M. Z., & Mahmud, S. (2019). *Landscape narrative of the Sundarban : Towards collaborative management by Bangladesh and India*, 1–207. http://documents.worldbank.org/curated/en/539771546853079693.

Ortolano, L., Sánchez-Triana, E., Paul, T., & Ferdausi, S. A. (2016). Managing the Sundarbans region: Opportunities for mutual gain by India and Bangladesh. *International Journal of Environment and Sustainable Development*, *15*(1), 16–31. https://doi.org/10.1504/IJESD.2016.073331

Paul, A. K., Ray, R., Kamila, A., & Jana, S. (2017). Mangrove degradation in the Sundarbans. *In Coastal Wetlands: Alteration and Remediation*, *21*, 357–392. https://doi.org/10.1007/978-3-319-56179-0_11

Payo, A., Mukhopadhyay, A., Hazra, S., Ghosh, T., Ghosh, S., Brown, S., Lázár, A. N., Bricheno, L., Wolf, J., Kay, S., Lázár, A. N., & Haque, A. (2016). Projected changes in area of the Sundarban mangrove forest in Bangladesh due to SLR by 2100. *Climatic Change*, *139*(2), 279–291. https://doi.org/10.1007/s10584-016-1769-z

Pham, T. D., & Yoshino, K. (2015). Mangrove mapping and change detection using multi-temporal Landsat imagery in Hai Phong city, Vietnam. *Paper presented at: The International Symposium on Cartography in Internet and Ubiquitous Environments* (Mar 17-19, 2015) Tokyo, Japan.

Pirotti, F., Laurin, G., Vettore, A., Masiero, A., & Valentini, R. (2014). Small footprint full-waveform metrics contribution to the prediction of biomass in tropical forests. *Remote Sensing*, *6*(10), 9576–9599. https://doi.org/10.3390/rs6109576

Quader, M. A., Agrawal, S., & Kervyn, M. (2017). Multi-decadal land cover evolution in the Sundarban, the largest mangrove forest in the world. *Ocean & Coastal Management*, *139*, 113–124. https://doi.org/10.1016/j.ocecoaman.2017.02.008

Rahman, M. M., Rahman, M. M., & Islam, K. S. (2010). The causes of deterioration of Sundarban mangrove forest ecosystem of Bangladesh: Conservation and sustainable management issues. *AACL Bioflux*, *3*(2), 77–90. http://www.bioflux.com.ro/aacl

Rahman, M. M. (2013). Temporal change detection of vegetation coverage in Patuakhali coastal area of Bangladesh Using GIS & Remotely Sensed Data. *International Journal of Geomatics and Geosciences*, *4*(36), 46.

Rahman, M. M., Khan, M. N. I., Hoque, A. F., & Ahmed, I. (2015). Carbon stock in the Sundarban mangrove forest: Spatial variations in vegetation types and salinity zones. *Wetlands Ecology and Management*, *23*(2), 269–283. https://doi.org/10.1007/s11273-014-9379-x

Rahman, M. M. (2020). Investigation into the Sea Level Rise as Fallout of Climatic Change: Case Study of the Coast of Bangladesh [M Phil. Dissertation], University of Dhaka. Retrieved March 7, 2022, from http://repository.library.du.ac.bd:8080/handle/123456789/1634

Ranson, M., Kousky, C., Ruth, M., Jantarasami, L., Crimmins, A., & Tarquinio, L. (2014). Tropical and extra-tropical cyclone damages under climate change. *Climate Change*, *127*(2), 227–241 https://doi.org/10.1007/s10584-014-1255-4

Roy, A. K. D., Alam, K., & Gow, J. (2013). Community perceptions of state forest ownership and management: A case study of the Sundarbans Mangrove Forest in Bangladesh. *Journal of Environmental Management*, *117*, 141–149. https://doi.org/10.1016/j.jenvman.2012.12.004

Roy, A., & Inamdar, A. B. (2019). Multi-temporal Land Use Land Cover (LULC) change analysis of a dry semi-arid river basin in western India following a robust multi-sensor satellite image calibration strategy. *Heliyon*, *5*(4), 1–20. https://doi.org/10.1016/j.heliyon.2019.e01478

Rwanga, S. S., & Ndambuki, J. M. (2017). Accuracy assessment of land use/land cover classification using remote sensing and GIS. *International Journal of Geosciences*, *8*(4), 611–622. https://doi.org/10.4236/ijg.2017.84033

Samanta, S., Hazra, S., Mondal, P. P., Chanda, A., Giri, S., French, J. R., & Nicholls, R. J. (2021). Assessment and attribution of Mangrove forest changes in the Indian Sundarbans from 2000 to 2020. *Remote Sensing*, *13*(24), 4957. https://doi.org/10.3390/rs13244957

Serrano, P. M. L., Rivas, J. J. C., Varela, R. A. D., González, J. G. A., & Sánchez, C. A. L. (2016). Evaluation of radiometric and atmospheric correction

algorithms for aboveground forest biomass estimation using landsat 5 TM data. *Remote Sensing*, *8*(5), 369. https://doi.org/10.3390/rs8050369

Smith, M. J. (2015). *A Comparison of DG AComp, FLAASH and QUAC Atmospheric Compensation Algorithms Using WorldView-2 Imagery*. Department of Civil Engineering Master's Report University of Colorado.

Stehman, S. V. (1996). *Estimating the kappa coefficient and its variance under stratified random sampling*. PE & RS. ASPRS, 401–407.

Talukdar, S., Singha, P., Mahato, S., Shahfahad, Pal, S., Liou, Y., & Rahman, A. (2020). Land-Use land-cover classification by machine learning classifiers for satellite observations-A review. *Remote Sensing*, *12*(7), 1135. https://doi.org/10.3390/rs12071135

Thakur, S., Maity, D., Mondal, I., Basumatary, G., Ghosh, P. B., Das, P., & Kumar De, T. (2021). Assessment of changes in land use, land cover, and land surface temperature in the mangrove forest of Sundarbans, northeast coast of India. *Environment, Development and Sustainability*, *23*(2), 1917–1943. https://doi.org/10.1007/s10668-020-00656-7

Tucker, C. J., Grant, D. M., & Dykstra, J. D. (2004). NASA's global orthorectified landsat data set. *Photogrammetric Engineering and Remote Sensing*, *70*(3), 313–322. http://dx.doi.org/10.14358/PERS.70.3.313

USGS. (2019). *LANDSAT COLLECTION 1 LEVEL 1 PRODUCT DEFINITION*. https://www.usgs.gov/media/files/landsat-collection-1-level-1-product-definition

Vaglio Laurin, G., Hawthorne, W., Chiti, T., Di Paola, A., Cazzolla Gatti, R., Marconi, S., Noce, S., Grieco, E., Pirotti, F., & Valentini, R. (2016). Does degradation from selective logging and illegal activities differently impact forest resources? A case study in Ghana. *IForest - Biogeosciences and Forestry*, *9*(3), 354–362. https://doi.org/10.3832/ifor1779-008

Varotsos, C. A., Efstathiou, M. N., & Cracknell, A. P. (2015). Sharp rise in hurricane and cyclone count during the last century. *Theoretical Applied Climatology*, *119*(3–4), 629–638. https://doi.org/10.1007/s00704-014-1136-9

Walsh, K. J., McBride, J. L., Klotzbach, P. J., Balachandran, S., Camargo, S. J., Holland, G., Knutson, T. R., Kossin, J. P., Lee, T., Sobel, A., & Sugi, M. (2016). Tropical cyclones and climate change. *Wiley Interdisciplinary Reviews. Climate Change*, *7*(1), 65–89. https://doi.org/10.1002/wcc.371

Zhang, K., Dong, X., Liu, Z., Gao, W., Hu, Z., & Wu, G. (2015). Mapping tidal flats with landsat 8 images and google earth engine: A Case Study of the China's Eastern Coastal Zone circa. *Remote Sensing*, *11*(8), 924. https://doi.org/10.3390/rs11080924